数理解析研究所講究録
第2048巻 2017年 19-25

Turbulent Reconnection And Compressible Magnetohydrodynamic Turbulence in Relativistic Plasmas

Makoto Takamoto

Department of Earth and Planetary Science, The University of Tokyo, Hongo, Bunkyo-ku, Tokyo, 113-0033, Japan

mtakamoto@eps.s.u-tokyo.ac.jp

1. Introduction

Magnetic reconnection is known as a process responsible for a very efficient magnetic field dissipation in many plasma phenomena. In particular, it is expected to play an important role for the acceleration of relativistic outflow in high energy astrophysical phenomena accompanying Poynting-dominated plasmas (Begelman et al. 1984; Kennel & Coroniti 1984a,b; Lyutikov & Blandford 2003). However, the classical theory of magnetic reconnection (Sweet 1958; Parker 1957) predicts that magnetic reconnection becomes very slow in high magnetic Reynolds number plasmas ($R_{\rm m} \sim 10^{10}$), and fails to explain observed dissipation timescale in space and astrophysical phenomena. To solve this problem, a lot of efforts have gone into finding a *fast-reconnection* process that does not depend on the value of resistivity. Using the equation of continuity, the reconnection rate can be expressed as

$$\frac{v_{\rm in}}{c_A} = \frac{\rho_{\rm s}}{\rho_{\rm in}} \frac{v_{\rm s}}{c_A} \frac{\delta}{L}, \tag{1}$$

where the subscript "*in*" and "*s*" indicate the inflow and outflow region, respectively, $v_{\rm in}, v_{\rm s}$ are the inflow and outflow velocity, respectively, c_A is the Alfvén velocity, ρ is the mass density, δ is the sheet thickness, and L is the sheet length. This equation shows that fast reconnection processes can be obtained by increasing the density ratio: $\rho_{\rm s}/\rho_{\rm in}$, (Brunel et al. 1982), the outflow velocity: $v_{\rm s}/c_A$, and the aspect ratio of sheets: δ/L (Biskamp 1986; Shibata & Tanuma 2001; Loureiro et al. 2007; Takamoto 2013).

Turbulence has been considered as a key process that can accelerate magnetic field annihilation. In particular, many astrophysical objects are considered to be high Reynolds number plasma, and it is natural to assume those plasma are in a turbulent state. It was theoretically suggested that strong Alfvénic turbulence also increases the sheet aspect ratio, and the reconnection rate becomes independent of the resistivity (Lazarian & Vishniac

(1999), henceforth LV99). LV99 predicts the following expression of reconnection rate:

$$\frac{v_{\rm in}}{c_A} \simeq \min\left[\left(\frac{L}{l}\right)^{1/2}, \left(\frac{l}{L}\right)^{1/2}\right]\left(\frac{v_l}{c_A}\right)^2 \tag{2}$$

where l and v_l are the energy injection scale and velocity dispersion of turbulence at the injection scale, respectively. This was examined using magnetohydrodynamics (MHD) simulation (Kowal et al. 2009). However, the numerical work was limited only in the non-relativistic incompressible regime, and the relativistic work has been performed only very recently by the authors (Takamoto et al. 2015).

2. Simulation Setup

We modelled the evolution of a current sheet in a turbulent flow using 3-dimensional resistive relativistic magnetohydrodynamics (RRMHD). The initial current sheet is modelled by the relativistic Harris sheet (Hoh 1966; Kirk & Skjæraasen 2003)

whose magnetic field is expressed as

$$\mathbf{B} = B_0 \tanh[z/\lambda]\mathbf{e}_x + B_G \mathbf{e}_y, \tag{3}$$

where λ is the half-thickness of the initial sheet, and B_0 and B_G are the reconnecting magnetic field and guide field component, respectively. The pressure inside of the sheet is assumed to satisfy the pressure balance, and the upstream pressure is determined by the magnetization parameter $\sigma \equiv B^2/4\pi\rho h c^2$ where $h = 1 + (\Gamma/(\Gamma-1))(p/\rho c^2)$ is the specific enthalpy of relativistic ideal gas with $\Gamma = 4/3$, and p, ρ, c are the gas pressure, mass density, and the light velocity, respectively. The initial temperature is assumed uniform, $\Theta \equiv k_{\rm B}T/mc^2 = 1$, where $k_{\rm B}, m$ are the Boltzmann constant and particle rest mass, respectively.

The evolution of the plasma is calculated using a 3-dimensional RRMHD scheme developed by Takamoto & Inoue (2011) which solves the full RRMHD equations in a conservative fashion using the constrained transport algorithm. This allows us to treat the mass density, momentum, energy, and divergence of magnetic field to be conserved within machine round-off error. The resistivity, η, was assumed to be constant, typically $\eta/Lc = 10^{-4}$. We followed the similar simulation setup used in Kowal et al. (2009). The numerical box is assumed $[-L/2, L/2] \times [0, L] \times [-L, L]$ where $L = 20\lambda$. Note that the z-direction size of the numerical box is twice larger than x,y-direction to reduce the influence by turbulence on the reconnection inflow around z-boundaries. We divided the numerical box into the homogeneous numerical cells with size: $\Delta = L/512$. The timestep size is set as: $\Delta t = 0.1\Delta/c$. We set the periodic boundary condition in y-direction and free boundary condition x and z-direction.

In our model, we drive turbulence using a similar method described by Mac Low (1999). We add a divergence-free 3-velocity field, $\delta\vec{v}$, and an electric field determined consistently to the injected velocity at time intervals $\Delta t_{\rm inj}$ in a box region located around the current sheet: $[-l_x, l_x] \times [0, L] \times [-l_z, l_z]$ where l_x, l_z are a scale length that is sufficiently larger than the injected turbulence eddy scale; The velocity field is described as: $\gamma \delta v^i = \sum_{\vec{k}} P(k) \sin(\vec{k} \cdot \vec{x} + \phi^i_{\vec{k}})$ where γ is the Lorentz factor of the injected velocity, i covers $\{x, y, z\}$, and $\phi^i_{\vec{k}}$ is a random phase. The one-dimensional power spectrum of the velocity field is assumed flat, $k^2 P(k) \propto k^0$. In our model, the only Alfvén mode velocity is injected. The more detailed explanation is provided in (Takamoto et al. 2015).

3. Results

The left-panel of Figures 1 are the observed reconnection rates $v_{\rm R}$ which is measured using a method proposed by Kowal et al. (2009) (see Equation (13) in this paper); this allows us to measure the effective value of E_y/B_0 in the 3-dimensional case, which provides us a reconnection inflow velocity less contaminated by turbulent flows than the direct measure of inflow velocity, v_z . The top panel shows the reconnection rate with respect to the injected turbulent velocity in various kinds of magnetized plasmas. This shows that the turbulent reconnection rate shows 3 characteristic behaviors depending on the injected turbulent velocity $v_{\rm inj}/c_A$: (1) increasing region following LV99; (2) saturation region giving maximum rate; (3) decreasing region. When the injected turbulent velocity is sufficiently small, incompressible approximation can be applied, and the reconnection rate grows following Equation (2). On the other hand, when injected velocity becomes comparable to the Alfvén velocity, turbulence becomes compressible and the reconnection rate deviates from the incompressible theory. Interestingly, the injection velocity $v_{\rm inj}/c_A$ at the maximum rate becomes smaller as the magnetization parameter increases. We will discuss the relation of this tendency to the compressible effects in the next section. Note that the error bar in the panel seems decreasing with σ. We consider this is because the kinetic energy of turbulence becomes smaller comparing with the magnetic field energy as the magnetization parameter σ increases. This maximum reconnection rate also indicate that it will be possible to reach around 0.1 to 0.2 if injection scales are comparable to the sheet length as indicated by Equation (2). The dependence of reconnection rate on turbulent strength is reported in Takamoto et al. (2015). This showed the reconnection rate becomes independent of the plasma resistivity but only on the turbulent strength whose value is around $v_{\rm R}/c_A \sim 0.05$. and even comparable to the relativistic Petschek reconnection rate (Lyubarsky 2005).

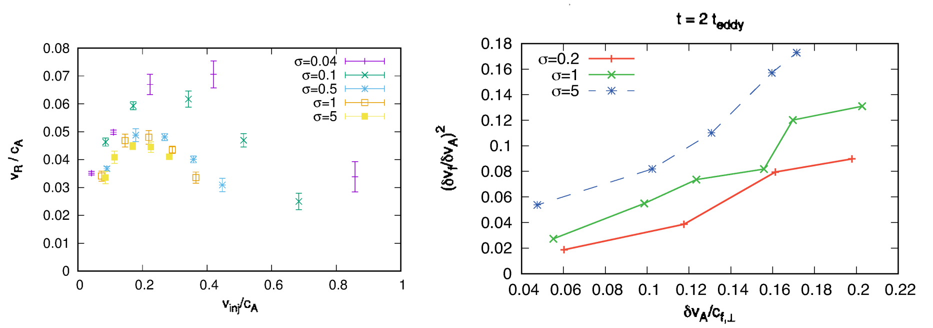

Fig. 1.— Left: Observed reconnection rate in its steady state. Reconnection rate with respect to the injected turbulent velocity. Right: The ratio of fast to Alfvén mode velocity power in terms of the non-relativistic fast Mach number of the Alfvén mode component. This indicates that the compressible mode increases with Alfvén Mach number, and becomes more important with increasing σ-parameter.

4. Theoretical Considerations

LV99 obtained the following relation: $\delta/L \propto (v_l/c_A)^2 \propto v_{\rm inj}/c_A$ using the incompressible MHD turbulence cascade law. Hence, in the present compressible RMHD turbulence case, it is expected the above relation should be modified. More precisely, the LV99's relation can be rewritten as:

$$\frac{\delta}{L} \sim \left(\frac{2\epsilon_{\rm inj} l}{c_A^3}\right)^{1/2} \min\left[\left(\frac{L}{l}\right)^{1/2}, \left(\frac{l}{L}\right)^{1/2}\right], \tag{4}$$

and substituting, $\epsilon_{\rm inj} \sim v_l^4/2lc_A$, recovers Equation (2). Hence, if we find an expression of the energy injection rate $\epsilon_{\rm inj}$ including compressible effects, Equation (4) may give us a new expression of the sheet width. Recently, Banerjee & Galtier (2013) obtained an exact relation of energy cascade rate in the non-relativistic isothermal MHD turbulence. In the strong background average magnetic field limit, the relation reduces to:

$$-4\epsilon = \nabla \cdot \vec{F} + B_0^2 S \tag{5}$$

where the divergence ∇ is performed on the correlation length which plays a role of the eddy scale length, $\vec{F}$ is the energy flux vector including compressible effects with order of B_0^2, and S is a source or sink term due to the compressible effects. This indicates that the compressible effects cannot be neglected in the strong background magnetic field, and the energy cascade rate should be redefined as an effective mean total energy cascade rate: $\epsilon_{\rm eff} \equiv \epsilon + B_0^2 S/4$, and this will give us the necessary correction term in Equation (4). Performing the Taylor expansion of $\epsilon_{\rm eff}$ in $v_{\rm inj}/c_A < 1$ up to 2nd-order, the corrected sheet width can be written as:

$$\frac{\delta}{L} \simeq \min\left[\left(\frac{L}{l}\right)^{1/2}, \left(\frac{l}{L}\right)^{1/2}\right]\left[\frac{v_{\rm inj}}{c_A} - C_1\left(\frac{v_{\rm inj}}{c_A}\right)^2\right], \tag{6}$$

where C_1 is a coefficient resulting from the expansion.

The 2nd-order correction, that decreases reconnection rate, can be explained as follows. The turbulent reconnection theory in LV99 considers the MHD turbulence results in a wider current sheet because of the wandering motion of the magnetic field driven by Alfvén waves. Hence, $\epsilon_{\rm inj}$ in Equation (4) is equivalent to the Alfvén wave power, V_A^2, where V_A is the Alfvén wave component of the velocity. In the compressible regime, a part of injected energy is distributed into the fast wave, and $\epsilon_{\rm inj}$ in Equation (4) should be rewritten as:

$$V_A^2 \simeq v_{\rm inj}^2 - V_f^2, \tag{7}$$

where V_f is the fast wave component of the velocity. The behavior of the fast mode V_f^2 is described in the right-panel of Figure 1, which shows the fast mode is actually a increasing function of Alfvén mode velocity, that is, injection velocity Takamoto & Lazarian (2016). More complete explanation is given in Takamoto et al. (2015). Interestingly, Takamoto & Lazarian (2016) also found that the fast mode component increases with the background Poynting energy. This indicates the critical-balance MHD would be invalid at some σ-value, and *a strong-coupling regime* between fast and Alfvén modes will appear around $\sigma \sim 10$.

5. Discussion And Conclusion

In this paper, we investigated turbulent reconnection in relativistic plasmas from the matter dominated to Poynting dominated cases using the relativistic resistive MHD model. The results show that the turbulence can enhance magnetic reconnection even in relativistic plasmas, and can be a candidate for a fast reconnection process. We found the reconnection rate in turbulence shows the following 3 characteristic phase depending on the velocity of the injected turbulence: (1) LV99 region (incompressible turbulence); (2) saturation region giving maximum rate; (3) reducing due to the compressibility. The saturation occurs when the compressible component become dominant, typically around $v_{\rm c}^2/v_{\rm i}^2 \gtrsim 0.4$ at which the maximum reconnection rate is about 0.05. This shows that the LV99 expressions for incompressible fluid should be modified to account for compressibility.

Finding a fast reconnection process is one of the most important topics in plasma physics, and a considerable number of studies have been conducted on it for a long time. Turbulence is a very general process in high-Reynolds number plasmas, so that turbulent reconnection can appear in many kinds of phenomena, such as astrophysical phenomena, nuclear fusion, and laser plasma. In particular, our work investigated the extension of turbulent reconnection to relativistic plasma with compressible turbulence, which allows us to apply this process to many high energy astrophysical phenomena, such as flares in pulsar wind nebulae, gamma ray bursts, and relativistic jets.

REFERENCES

Banerjee, S., & Galtier, S. 2013, Phys. Rev. E, 87, 013019

Begelman, M. C., Blandford, R. D., & Rees, M. J. 1984, Reviews of Modern Physics, 56, 255

Bhattacharjee, A., Huang, Y.-M., Yang, H., & Rogers, B. 2009, Physics of Plasmas, 16, 112102

Biskamp, D. 1986, Physics of Fluids, 29, 1520

Blandford, R. D., & Znajek, R. L. 1977, MNRAS, 179, 433

Brunel, F., Tajima, T., & Dawson, J. M. 1982, Physical Review Letters, 49, 323

Deng, W., Li, H., Zhang, B., & Li, S. 2015, ApJ, 805, 163

Eyink, G. L. 2011, Phys. Rev. E, 83, 056405

Higashimori, K., Yokoi, N., & Hoshino, M. 2013, Physical Review Letters, 110, 255001

Hoh, F. C. 1966, Physics of Fluids, 9, 277

Inoue, T., Asano, K., & Ioka, K. 2011, ApJ, 734, 77

Kennel, C. F., & Coroniti, F. V. 1984a, ApJ, 283, 694

—. 1984b, ApJ, 283, 710

Kino, M., Takahara, F., Hada, K., Akiyama, K., Nagai, H., & Sohn, B. W. 2015, ApJ, 803, 30

Kirk, J. G., & Skjæraasen, O. 2003, ApJ, 591, 366

Komissarov, S. S., Barkov, M. V., Vlahakis, N., & Königl, A. 2007, MNRAS, 380, 51

Kowal, G., Lazarian, A., Vishniac, E. T., & Otmianowska-Mazur, K. 2009, ApJ, 700, 63

Lazarian, A., & Vishniac, E. T. 1999, ApJ, 517, 700

Loureiro, N. F., Schekochihin, A. A., & Cowley, S. C. 2007, Physics of Plasmas, 14, 100703

Lyubarsky, Y., & Kirk, J. G. 2001, ApJ, 547, 437

Lyubarsky, Y. E. 2005, MNRAS, 358, 113

Lyutikov, M., & Blandford, R. 2003, ArXiv Astrophysics e-prints

Mac Low, M.-M. 1999, ApJ, 524, 169

Matthaeus, W. H., & Lamkin, S. L. 1985, Physics of Fluids, 28, 303

Parker, E. N. 1957, J. Geophs. Res, 62, 509

Shibata, K., & Tanuma, S. 2001, Earth, Planets, and Space, 53, 473

Sironi, L., & Spitkovsky, A. 2014, ApJ, 783, L21

Sweet, P. A. 1958, in IAU Symposium, Vol. 6, Electromagnetic Phenomena in Cosmical Physics, ed. B. Lehnert, 123

Takamoto, M. 2013, ApJ, 775, 50

Takamoto, M., & Inoue, T. 2011, ApJ, 735, 113

Takamoto, M., Inoue, T., & Inutsuka, S. 2012, ApJ, 755, 76

Takamoto, M., Inoue, T., & Lazarian, A. 2015, ApJ, 815, 16

Takamoto, M., & Lazarian, A. 2016, ArXiv e-prints

Uzdensky, D. A., Loureiro, N. F., & Schekochihin, A. A. 2010, Physical Review Letters, 105, 235002

Zhang, B., & Yan, H. 2011, ApJ, 726, 90

This preprint was prepared with the AAS LaTeX macros v5.2.